Int. J. Electrochem. Sci., 12 **(2017)** 8847 – 8859, doi: 10.20964/2017.10.45

International Journal of
ELECTROCHEMICAL
SCIENCE
www.electrochemsci.org

Sensitive Electrochemical Measurement of Thiamethoxam on Nanocomposite Coated Carbon Paste Using FFT Coulometric Admittance Voltammetry and Flow Injection Analysis

Parviz Norouzi[1,2,*] *Nazanin Ghaheri*[1], *Mostafa Aghazadeh*[1], *Zahra Mofidi*[1], *Bagher Larijani*[3,*]

[1] Center of Excellence in Electrochemistry, School of Chemistry, College of Science, University of Tehran, Tehran, Iran
[2] Biosensor Research Center, Endocrinology & Metabolism Molecular-Cellular Sciences Institute, Tehran University of Medical Sciences, Tehran, Iran
[3] Endocrinology & Metabolism Research Center, Endocrinology & Metabolism Molecular-Cellular Sciences Institute, Tehran University of Medical Sciences, Tehran, Iran
*E-mail: norouzi@khayam.ut.ac.ir; emri@tums.ac.ir

Received: 30 June 2017 / *Accepted:* 7 August 2017 / *Published:* 12 September 2017

The object of this work was to study of the application of a new sensor for determination of Thiamethoxam using Fast Fourier transform Coulometric Admittance Voltammetry (FFTCAV) in a flow-injection analysis. The sensor was constructed by casting mixture of chitosan, multi-walled carbon nanotubes, reduced graphene nanosheets and Au nanoparticles on a carbon paste ionic liquid electrode. The application of nanoparticles created an environment for amplification of the analyte admittance. Also, the sensitively of the measurement was achieved by integration of the sensor admittance in specific potential range, after background subtraction. The characterization of the sensor surface was studied by scanning electron microscopy and electrochemical impedance spectroscopy methods. The results showed that the sensor response was proportional to concentrations of Thiamethoxam in range of 0.5×10^{-10} to 350 $\times10^{-10}$ M with a detection limit of 6.2×10^{-12}M. The technique exhibited a good reproducibility and accuracy. Moreover, the constructed sensor exhibits a long-term of usage stability.

Keywords: FFT Coulometric Admittance Voltammetry, Thiamethoxam, Au nanoparticles, Ionic liquid

1. INTRODUCTION

Thiamethoxam is a systemic insecticide in the class of neonicotinoids [1]. It has been extensively used in the agriculture industry due to its advantages, such as high activity against pests and insects [2, 3]. The biological activity of neonicotinoids is ascribed to their interference on the nicotinic acetylcholine receptors and therefore they exhibit specific activity against the insect nervous system [4, 5]. This form of activity makes these compounds highly applicable to control the biological effect of insects, in cases when the insects develop resistance to conventional organophosphate, carbamate and pyrethroid insecticides [6]. Fig. 1 shows the chemical structure of Thiamethoxam.

Moreover, Thiamethoxam is highly soluble in water systems and thus the wide application of this plant protecting agent in many countries may present a threat to environmental safety and human health [7]. Therefore, rapid and sensitive determination of this insecticide in environmental waters is significantly critical. Numerous methods have been applied for determination of Thiamethoxam involved high-performance liquid chromatography (HPLC) [8, 9], mass spectrometry [10, 11], enzyme-linked immunosorbent assay [12], Fourier transform infrared spectrometry [13] and electrochemical methods in which modified electrodes were used [14, 15]. Due to simplicity and low cost, there is a grate tendency to develop more accurate and sensitive electrochemical technique and sensors.

Modified electrodes have obvious advantages for electrochemical detection of different analytes. For example, in different modified electrodes, ionic liquids (IL) has be used wildly due to its conductivity which facilities the electron transfer and decreasing the over potential for biomolecules redox reaction and enhance the electrochemical signals [16]. Also, IL has shown good stability and well biocompatibility, and it can be used as the binder in carbon paste electrodes in order to improve the performance of the carbon paste electrodes. These electrodes, which are called carbon ionic liquid electrodes (CILEs), have established specific characteristics, including increased reversibility, higher sensitivity and wider electrochemical windows [16-18]. On the other hand, different kind of nanomaterials such as nanoparticles (NPs), multi-walled carbon nanotubes (MWCNTs) and reduced graphene nanosheets (RGNS) have been widely used for modification of the electrodes for various electrochemical applications due to their high surface area and rapid heterogeneous electron transfer which accelerates the electrochemical reaction rate [19-34].

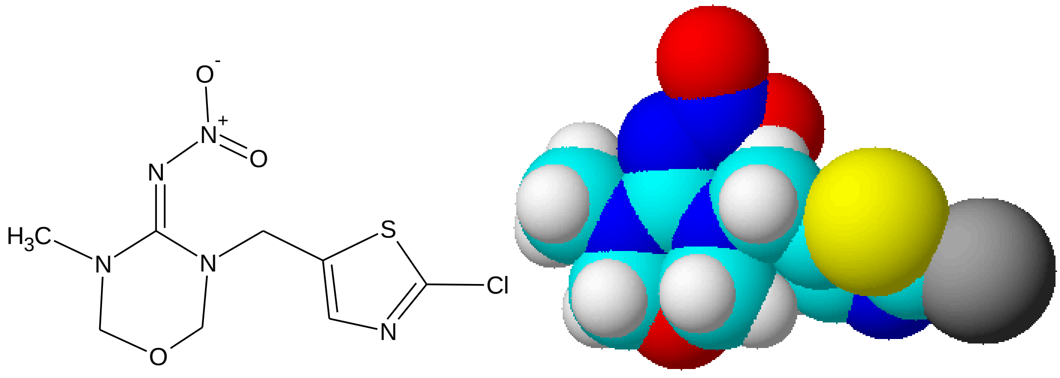

Figure 1. Structure of Thiamethoxam

In this study FFT Coulometric Admittance Voltammetry (FFTCAV) technique was used to investigate the electrochemical response of Thiamethoxam on the surface of a new sensor in a flow injection analysis system [35-41]. The scanning electron microscopy (SEM) and electrochemical impedance spectroscopy (EIS) methods were used to characterize the surface of the sensor. Under the optimal conditions, the integrated admittance signal of the electrode in a selected potential range was recorded as the sensor response to analyte. The electrocatalytic property of the developed sensor was demonstrated a good behavior for electrochemical determination of Thiamethoxam.

2. MATERIALS AND METHODS

2.1. Reagents

All chemicals and solvents used were of analytical grade and were used as received. Thiamethoxam was purchased from Sigma–Aldrich. Chitosan and $HAuCl_4$ were purchased from Shanghai Chemicals (Shanghai, China). Graphene nanosheets was purchased from Sinopharm Henan Bonzer Imp (China). Multi-walled carbon nanotubes was purchased from Hongwu International Group (Hong Kong). All other chemicals were purchased from Sigma–Aldrich. The standard solutions were prepared in double distilled water. The stock solution of 2mM of Thiamethoxam was firstly prepared, and then an aliquot was diluted to the appropriate concentration.

2.2. The sensor fabrication

For preparation of the ionic liquid carbon paste electrode (CILE), 5 g of graphite powder and 2 g of IL were hand-mixed thoroughly in a mortar and heated at a temperature of 100 °C to form a homogeneous mixture. The paste was packed into a Teflon tube (i.d. 4mm). Then, a copper wire installed into the paste as the electrical contact and the electrode was left to cool to the room temperature. Finally, by smoothing the electrode onto a weighing paper a mirror-like surface was obtained. For obtaining RGNS/CILE, at first, GNSO was prepared by a modified Hummers method using expandable graphite flake as the original material [42]. Then, through a chemical reduction of 1.0 mg/mL GNSO powder in distilled water with 150 mM $NaBH_4$ and then mixture was kept at 90 °C for 30 min to obtain RGNS. The product was centrifuged to precipitate the RGNS powder, which was eventually dried in vacuum at low temperature [43]. Then, RGNS was, then added to10 mL methanol (to produce 1.5 mg/mL of RGNS) and sonicated for 30 min. Then the mixture solution was cast on the surface of CILE and left it to dry at room temperature to form a stable film. For the next modification step, 100 ml of 0.01% $HAuCl_4$ solution was brought to boiling with vigorous stirring, and then 2.5 ml of 1% sodium citrate solution was quickly added to give a red-violet color. Boiled for additional 10-12 min, then the heater was removed and the resulting mixture was stirred continuously for another 10 min [44]. The cooled Au NPs colloid solution was stored at 4 °C in a dark bottle. 10µL of the Au NPs colloid solution was casted on RGNS/CILE and was dried at room temperature for about 1 h. To obtain MWCNT/AuNP/RGNS/CILE, the MWCNT ethanolic solution (1.5 mg/mL) was casted on the surface of AuNP/RGNS/CILE. Finally, 20µL of the 2% chitosan solution in acetic acid was casted on MWCNT/AuNP/RGNS/CILE and allowed to dry at room temperature for about 1 h. CHI-

MWCNT/AuNP/RGNS/CILE was obtained and could be used after washing with distilled water. The schematic diagram of the electrode preparation is shown in Fig. 2.

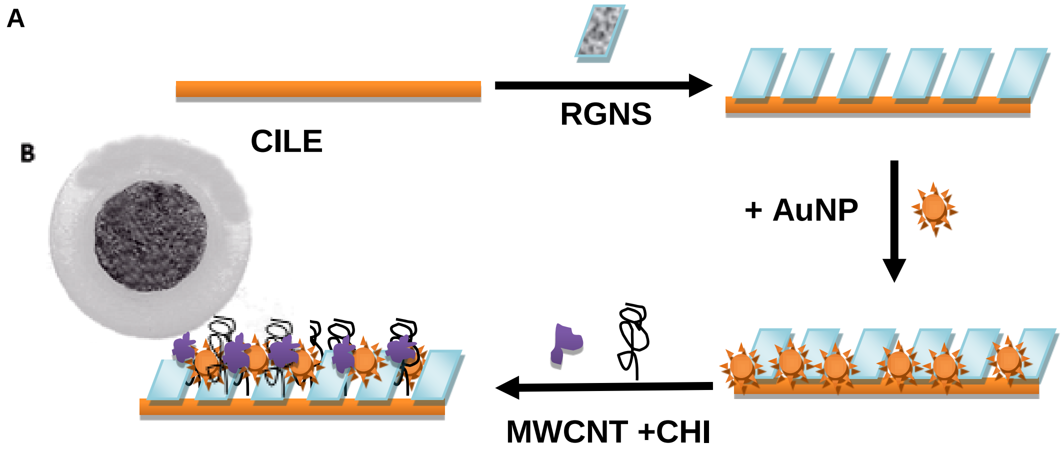

Figure 2. A) Schematic diagram of the constructed Sensor, B) The Teflon tube filled with the paste.

2.3. Apparatus

The equipment was used a flow injection analysis system consist of an eight roller peristaltic pump (UltrateckLabs Co., Iran) and a four way injection valve (UltrateckLabs Co., Iran,) with a 600 µL sample injection loop (Inset the diagram of the electrochemical cell).

The electrochemical FFTCAV was carried out with a homemade potentiostat, which was connected to a PC equipped with an analog to digital data acquisition board (PCL-818H, Advantech Co.). The program was used to generate an analog waveform and acquire current readings. As presented in Fig 3, the potential waveform has a multiple SW cycles with amplitude of E_{sw} and frequency of f_o, which were superimposed on a staircase potential function whit a small potential step of ΔE (10 mV). The value of E_{sw} was in the range of 5 to 45 mV. Also, as shown in the figure, during the potential ramp, the currents were sampled eight times per each SW cycle. The potential waveform was repeatedly applied to the working electrode and then the data was acquired and stored by the software. Furthermore, the program was able to process and plot the data in real time. The electrochemical program was used to generate an analog waveform and acquire current readings.

Electrochemical impedance spectroscopy (EIS) measurements were performed in a faraday cage with AutoLab Potentiostat PGSTAT302N (Metrohm AutoLab BV, U) in 3 mM $[Fe(CN)_6]^{3-/4-}$ solution in 0.1M KCl.

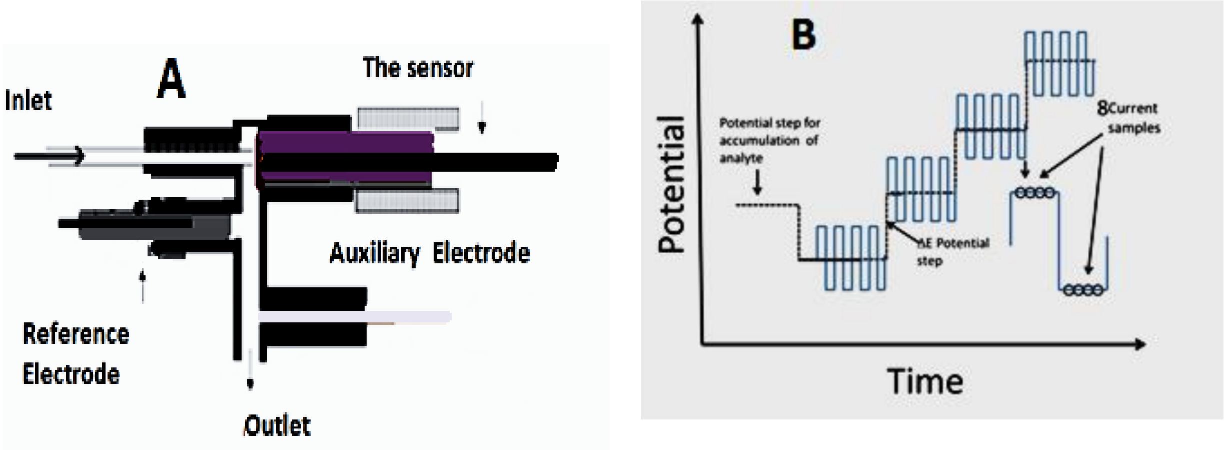

Figure 3. The applied potential waveform for FFTCAV. Inset diagram shows the electrochemical cell.

3. RESULTS AND DISCUSSION

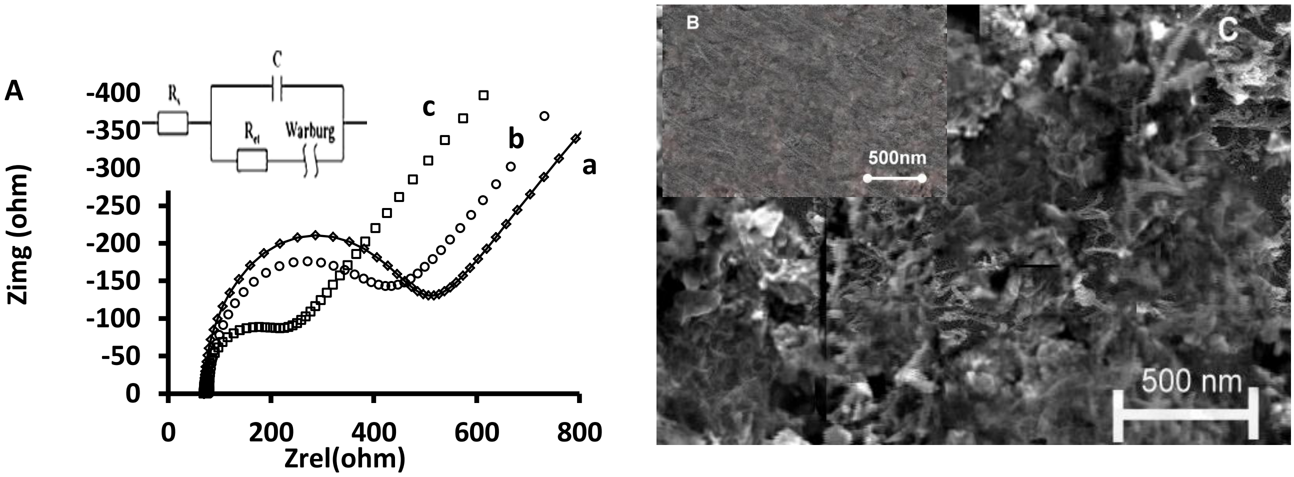

Figure 4. A) Nyquist plots of the modified electrodes in 3 mM $K_3Fe(CN)_6$ solution in 0.1 M KCl: (a)bare CILE, (b)AuNP/RGNS/CILE, (c)CHI-MWCNT/AuNP/RGNS/CILE, B) SEM image of CILE and C)SEM image of CHI-MWCNT/AuNP/RGNS/CILE

Fig. 4A demonstrates EIS plots for the unmodified CILE, AuNP/RGNS/CILE and CHI-MWCNT/AuNP/RGNS/CILE in 0.1 M KCl solution containing 3 mM $[Fe(CN)_6]^{3-/4-}$. The equivalent electrical circuit is shown in the inset in Fig. 4A. The results showed that the R_{ct} (which is the charge transfer resistance) of AuNP/RGNS/CILE (curve b) was lower than that was obtained for the bare CILE electrode. This suggests that the combination of Au NP and RGNS encompass an excellent electrical conducting materials, which could decrease the resistance of the electrode surface. Likewise, the decrease of the value of R_{ct} for CHI-MWCNT/AuNP/RGNS/CILE is shown in curve c. This is an indication of enhancement of the conductivity and higher collection of $[Fe(CN)_6]^{3-/4-}$ species on the sensor surface, which can enhance the value of the current of $[Fe(CN)_6]^{3-/4-}$.

Figures 4 B and C show the SEN images of CILE and CHI-MWCNT/AuNP/RGNS/CILE, respectively. The SEM image of CILE appear a uniform surface without the separated carbon layers. Meanwhile, due to hydrophilic with higher viscosity of IL the gaps, in the layers of graphite powder, could be sealed that connects the isolated carbon flask. This could help to create a flat surface for the sensor. Figure C shows the formed structure for CHI-MWCNT/AuNP/RGNS/CILE is in a range of nanometers, which could form a large surface area and higher attachment sites on the film for the analyte. The images reveals the average size of Au NPs is 40 nm, in which the distribution of Au NPs is in MWCNT/RGNS is uniform. In fact, formation of MWCNT/RGNS/CILE layer on the surface of CILE is necessary to reach higher surface area to generate a good porosity and stabilized Au NPs on the surface.

3.1. Electrochemical technique

For determination of Thiamethoxam, the admittance of the sensor was calculated during the potential scans. Fig.5 shows FFTCAV signals and the changes in form of differential admittance for the sensor in the potential range of -100 to -1000 mV, at SW frequency 300 Hz and amplitude 25mV. As mentioned above, in FFTCAV technique the current is sampled eight times, across the entire SW period, and the current were used to calculate the differential admittance during continuous ramps [34, 39, 45-51]. The potential axis in the graph represents potential applied to the working electrode during potential scan and the time axis represents the time of a experiment run. Meanwhile, in this graph the first admittance voltammogram (as reference voltammogram) was subtracted from the subsequent voltammograms and therefore all admittance values were set to zero, before injection of the analyte. As results, as shown, for each injection, a peak appears at the potential of -810 mV, which is due to the reduction of Thiamethoxam on the sensor surface.

One of the advantages of scanning approaches for electrochemical detection is that most sensitive part of the voltammogram could be selected for integration of admittance in order to calculate the detector response. Here, the admittance integration by voltage results in form of columbe (C), and the electrode response is called ΔQ. The value of ΔQ is calculated based on the equations 1 and 2:

$$\mathit{\Delta} Q = \mathrm{Q} - \mathrm{Q}_0 \qquad (1)$$

$$\Delta Q\ (n\tau) = \Delta t \left[\sum_{E=E_1}^{E=E2} \left| A(s,E).E - \sum_{E=E}^{E=E2} A(s_r,E).E \right| \right] \qquad (2)$$

where Q is the electrical charge obtained by integration of admittance voltammetric curve between E_i and E_f, and Q_0 represents Q in the absence of the analyte. *n* is the sweep number, τ is the time period between subsequent sweeps, *Δt* is the time difference between two subsequent points on the FFTCA voltammogram, *A* (*n, E*) represents the value of admittance of measured during the n^{th} scan and A(n_r, *E*) is the reference admittance in the voltammogram. E_i and E_f are the initial and the final potential range of integration, respectively. The reference *FFTCAV* curve was obtained by averaging 5 FFTCAV curves recorded at the beginning of the experiment (i.e. before injection of the analyte). The inset of Fig. 5 illustrates the calculated response for CHI-MWCNT/AuNP/RGNS/CILE toward the injection of 5.0×10^{-7} M of Thiamethoxam. In this technique, coulometric signal is calculated based on the integration of the admittance changes in a potential range at the voltammograms. The results specify that with increasing the concentration of Thiamethoxam in the injected sample, ΔQ increases proportionally. Also, it should be remarked that in this technique, all of the electrochemical processes that may occur for the analyte, potentially carry useful analytical information. For example, absorption and the redox reaction of analytes could create charging and faradic admittance responses.

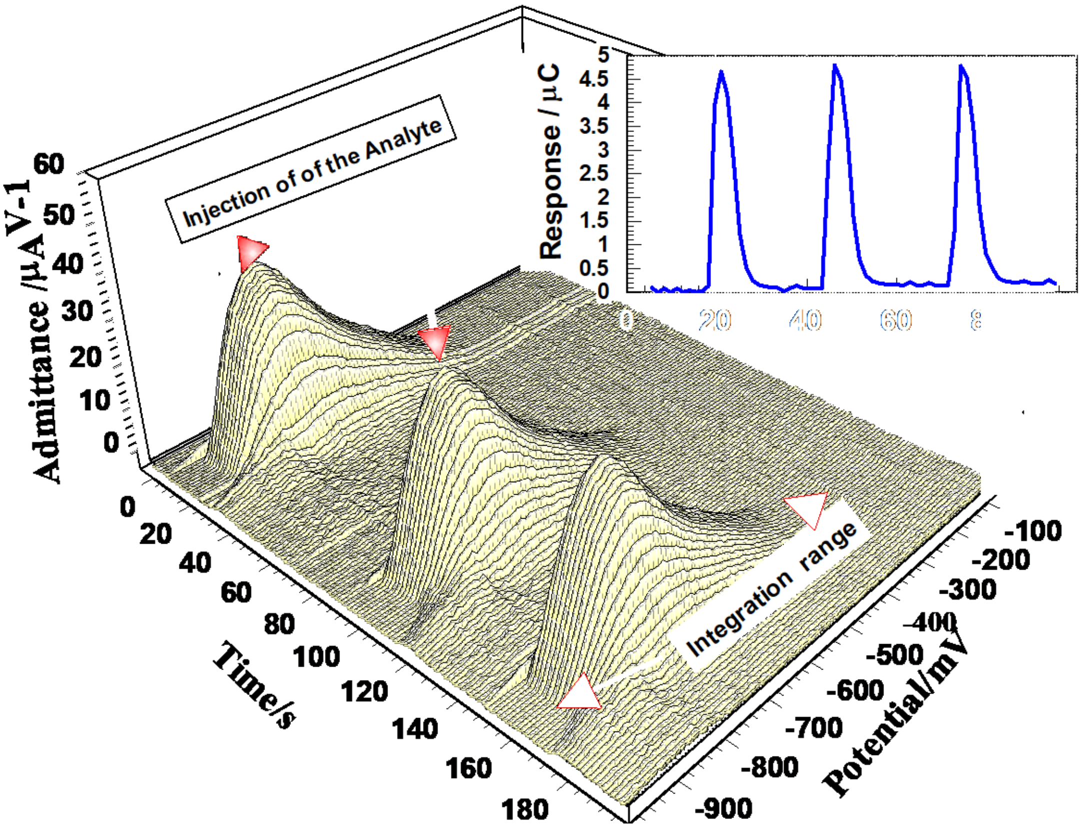

Figure 5. FFT admittance voltammograms of the CHI-MWCNT/AuNP/RGNS/CILE in absence and after injection of 5.0×10^{-8} M Thiamethoxam in the phosphate buffer solution at pH 8.5; at frequency 300 Hz and amplitude 25mV. The inset shows the calculated response from the voltammograms, integration potential range for the admittance is -300 to -900 mV.

As shown in Fig. 2, it is advantageous in FFTCAV technique to collect more current samples near the end of the forward and reverse SW pulses for signal averaging to increase the S/N. In addition, by optimizing important factors in the electrochemical detection, the S/N response could be maximized.

3.2. Optimization of SW frequency and amplitude

It is well known that in a voltammetric measurement, condition of the applied potential waveform has effect on the response of the sensor and background noise. Accordingly, it can be expected that the FFTCAV response of the analyte depends on the applied SW frequency (f_o.) and amplitude (E_{sw}) for the potential waveform. To find the optimum SW waveform condition, the f_o. and E_{sw} were examined in range 50-700 Hz and 5 to 50 mV, respectively. Fig. 6 shows the three dimensional graph for change in the analyte response (ΔQ) respect to the assigned changes in E_{sw} and f_o. The value of ΔQ was calculated in integration potential range -300 to-900 mV and the concentration of the injection sample was 2.0×10^{-8} M of Thiamethoxam in buffer solution at pH 8.5.

As shown in the figure the admittance of the sensor increases, as well as, the value of *ΔQ* with f_o up to 300 Hz. A similar behavior can be seen for the enhancing the amplitude up to 25 mV. This could be due to this fact that f_o. and E_{sw} play similar roles that sweep rate has cyclic voltammetry. Therefore, the increase in the speed of excitation waveform can cause an enhancement in the value of the Thiamethoxam response. The figure, also, illustrates that the value of ΔQ decreases after the frequency of 300 Hz and the amplitude of 25mV, which can be attributed to the solution resistance and generation higher capacitance current (or noise) of the system. Also, it can be suggested that applying higher values of f_o. and E_{sw} can limit the time window of the electrochemical processes , which consequently limits the kinetic of the electrode processes.

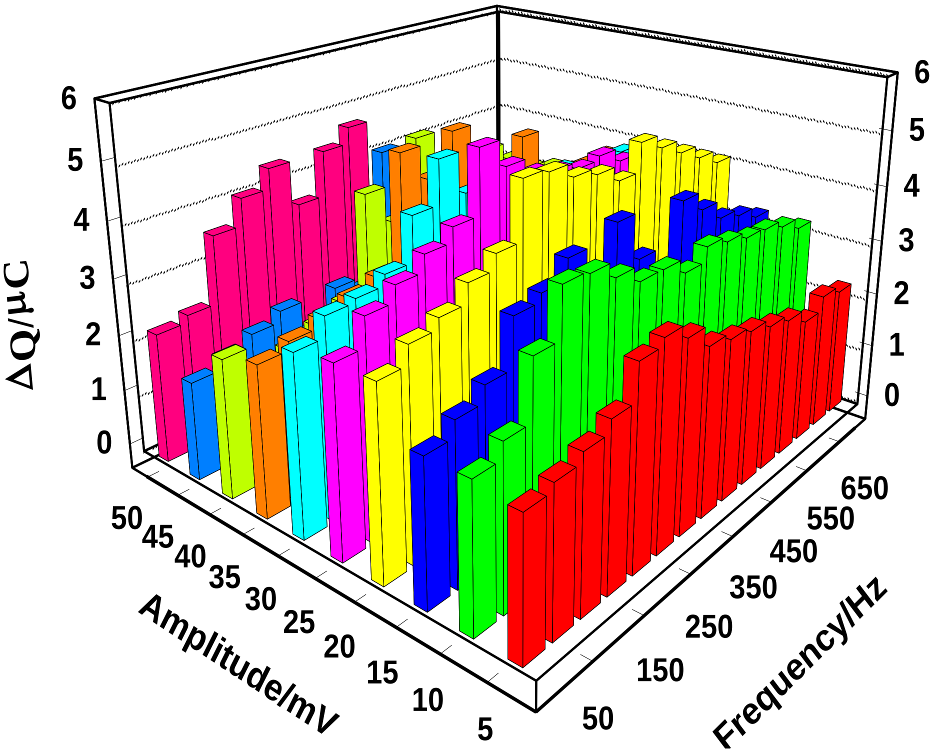

Figure 6. The effect of frequency and amplitude on the sensor response to injection of 2.0×10^{-8} M Thiamethoxam in the buffer solution at pH 8.5; for the scanned potential range of -100 to -1000 mV. The integration potential range for the admittance was -300 to-900 mV

3.3. Effect nanoparticles in the sensor fabrication

Fig. 6 shows the effect of amount of MWCNT and RGNS in CHI-MWCNT/AuNP/RGNS/CILE on the sensor response. The injected solution was 2.5 $\times 10^{-8}$ M Thiamethoxam in the buffer solution at pH 8.5 and FFACVs were recorded at frequency 300Hz and amplitude 25mV. The three dimensional graph reveals the dependence of the sensor response on the amount of RGNS and MWCNT in the content of the modifier or film composition. The examination were done with different volume of solutions of RGNS and MWCNT suspension solution, which was casted on the CILE surface. In these measurements, volumes of solution of RGNS and MWCNT were in range of 4 to 40 µL and 4 to 25 µL (with constant amount of Au NPs). For calculating the response, the integration potential range was -300 to -900 mV.

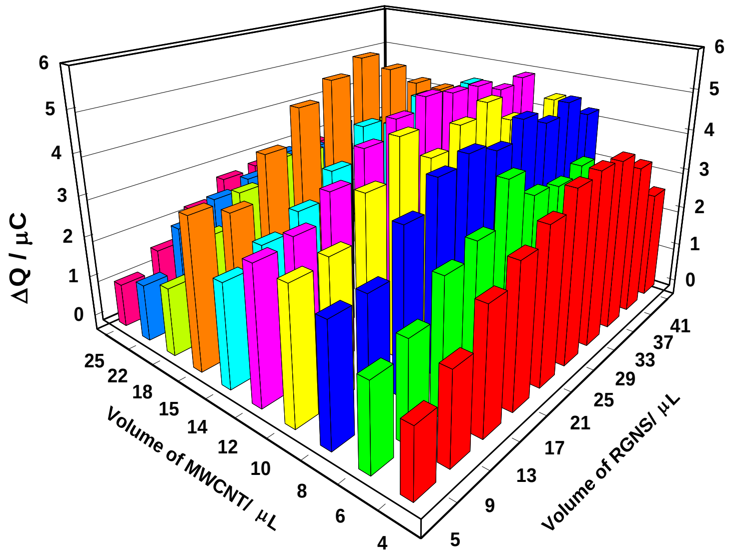

Figure 7. The effect of amount of MWCNT and RGNS in CHI-MWCNT/AuNP/RGNS/CILE on the sensor response to 2.5×10^{-8} M of Thiamethoxam in the buffer phosphate solution at pH 8.5, in the potential range of -300 to -900mV at frequency of 300Hz and amplitude 25mV.

The graph indicates that the value of *ΔQ* increases with RGNS volume up to 25µL and then it decreases slightly. Moreover, as shown in figure, in the case of MWCNT the value of *ΔQ* enhances with the volume of the MWCNT, in the composition, up to 18 µL, whereas, *ΔQ* drops slightly after that casted volume. The reduction in the response could be due to the reduction of the active sites of the surface of the sensor by filling the spaces or holes, which could increase the resistance of the surface of the electrode.

3.4. Calibration curve

To evaluate the reproducibility and sensitivity the sensor toward the Thiamethoxam concentration, a series of five prepared electrodes were used in the measurements. Also, a set of standard solution of analyte were made in a range of 0.5×10^{-10} to 350 $\times10^{-10}$ M in the buffer phosphate solution at pH 8.5. The FFTACV measurements were done in the potential range of -100 to -1000 mV at frequency of 300 Hz and amplitude of 25mV.

In addition, the FFTCAV determination of Thiamethoxam was established on the change in the sensor ΔQ after injection of the standard solutions. Fig. 8 illustrates a typical ΔQ response of the CHI-MWCNT/AuNP/RGNS/CILE to a set of standard solutions of Thiamethoxam, where ΔQ was calculated based on equation 2 in a selected potential range (-300 to -900 mV). In this figure, each point represents the average of 3 signal for of Thiamethoxam, under optimal conditions.

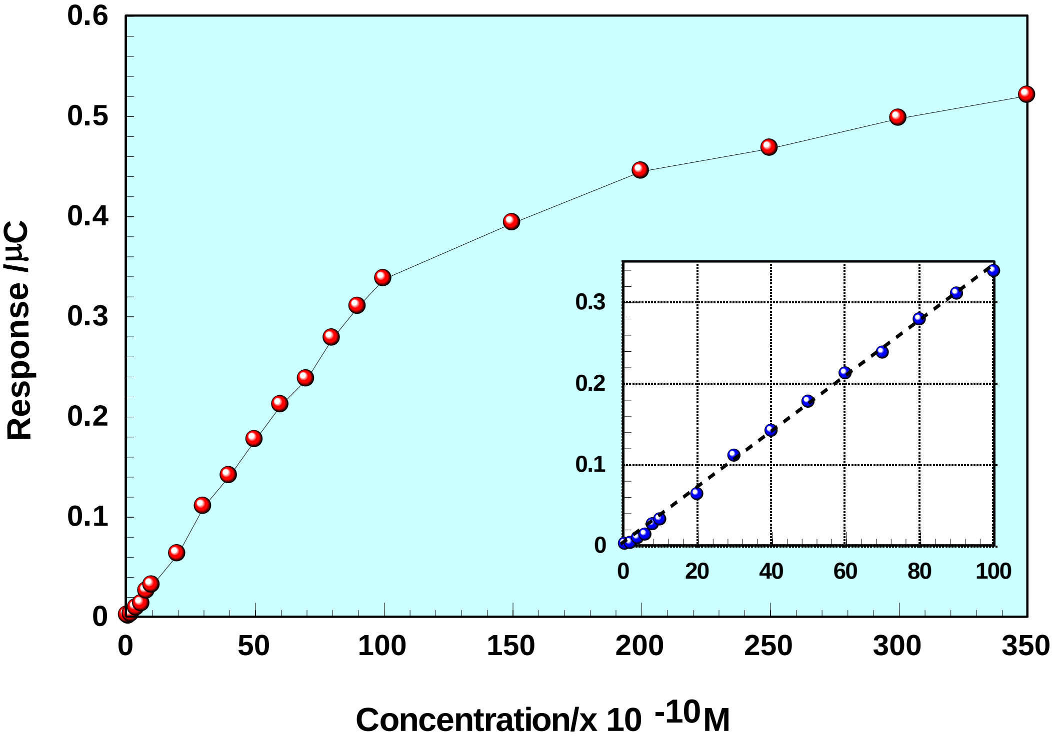

Figure 8. Response of the CHI-MWCNT/AuNP/RGNS/CILE to different concentrations of Thiamethoxam in the buffer phosphate solution at pH 8.5, in the potential range of -200 to -900mV at the frequency of 300Hz and amplitude of 25mV.

The results showed the relative standard deviation (RSD) of the measurements for five electrodes was 1.97%, suggesting that the precision and reproducibility of the proposed detection technique was quite promising. As shown in the inset graph in Fig. 8, the analyte response has a linear range of 0.5×10^{-10} to 100 $\times10^{-10}$ M with correlation coefficient of 0.998. The estimated detection limit (DL) based on signal to noise ratio ($DL=y_B+3s_B$,) was found 6.2×10^{-12}M. The DL of the electrochemical technique has been compared with some other of the best previously reported such as HPLC, mass spectrometry, enzyme-linked immunosorbent assay and Fourier transform infrared spectrometry [8-13]. Moreover, in case electrochemical detection, although DL of the technique is not the lowest compared with mass spectrometry methods, but, the linear range is widest which is a benefit for future practical application in development portable devices. Thiamethoxam measurement based on the utilization of different materials as the sensor and different detection techniques (Table 1) and it was confirmed that the presented sensor with FFTCAV exhibited an excellent and reproducible sensitivity [14, 52-57]. The comparison in the table is clearly highlighted the remarkable decline in DL for FFTCAV. A long term storage stability of the CHI-MWCNT/AuNP/RGNS/CILE was tested for 90 days, and it was seen that the sensitivity retained 97.6%. This indicates that, the proposed technique is more reproducible, by means of application of a simple paste electrode, than other methods.

Table 1. The comparison of the proposed sensor with the best previous reported ones based on the utilization of different materials and different detection techniques.

Detection method	**DL**	**Materials**	**Ref**
Differential pulse voltammetry	12 μM	Tricresyl phosphate-based carbon paste electrode	[14]
Cyclic voltammetry	29 μ M	Glassy carbon electrode	[52]
Differential pulse voltammetry	1.3 μM	Bismuth film modified glassy carbon electrode	[53]
Differential pulse voltammetry	0.1 μM	Nanosilver/SDS modified glassy carbon electrode	[54]
Square-wave voltammetry	0.6 μM	Silver-amalgam film electrode	[55]
Differential pulse voltammetry	0.36 μ M	Modified silver solid amalgam	[56]
Differential pulse voltammetry	8.3 μM	Graphene oxide modified electrodes	[57]
FFTCAV	6.2×10^{-6} μM	CHI-MWCNT/AuNP/RGNS/CILE	This work

4. CONCLUSIONS

This paper presented that the AuNP-CHI/MWCNT/RGNS/CILE nanocomposite can provide a unique microenvironment for the direct electrochemistry of Thiamethoxam in flow injection analysis. Also, application of FFTCAV technique provides a novel electrochemical producer for Thiamethoxam measurement, which is sensitive and promising. It should be noted that in this technique, all electrochemical processes involving absorption and redox reaction of Thiamethoxam on the electrode surface contribute in changing admittance of the analyte, which can enhance the sensitivity of measurements. This is the special ability of FFTCAV technique which collects more data current samples near the end of the forward and reverse pulses and utilization signal averaging to increase the S/N. Also, the increased S/N can be attributed to the synergy effect of RGNS and AuNPs on the oxidation of Thiamethoxam. It can be suggested that the sensor has excellent responses because of the large surface area and fast electron transfer on graphene. In addition, the electrochemical technique reveals some other excellent characteristics such as wide linear range, low detection limit and relatively long-term stability for 90days. As well, the proposed sensor has easy fabrication and low cost. The sensitized recognition based on combination nanocomposite sensor and FFTCAV technique provides a new strategy for determination of drug molecules in flowing solution, such as chromatography.

ACKNOWLEDGEMENT
The authors are grateful to the Research Council of University of Tehran for the financial support of this work.

References

1. R. Nauen, , U. Ebbinghaus-Kintscher, V.L. Salgado, and M. Kaussmann, Pesticide *Biochemistry and Physiology*, 76 (2003) 55.
2. P. Maienfisch, M. Angst, F. Brandl, W. Fischer, D. Hofer, H. Kayser, W. Kobel, A. Rindlisbacher, R. Senn, and A. Steinemann, *Pest Management Science*, 57 (2001) 906.
3. A. Pozzebon, C. Duso, P. Tirello, and P.B. Ortiz, *Pest Management Science*, 67 (2011) 352.
4. A. Elbert, M. Haas, B. Springer, W. Thielert, and R. Nauen, *Pest Management Science*, 64 (2008) 1099.
5. P. Jeschke, and R. Nauen, *Pest Management Science*, 64 (2008) 1084.
6. G.W. Ware, and D.M. Whitacre, MeisterPro information resources, a division of Meister media worldwide, 4th edn. Willoughby, Ohio, USA, 2004.
7. S.T. Kurwadkar, D. Dewinne, R. Wheat, D.G. McGahan, and F.L. Mitchell, *Journal of Environmental Science and Health*, Part B, 48 (2013) 237.
8. J. Vichapong, R. Burakham, and S. Srijaranai, *Talanta*, 139 (2015) 21.
9. E. Watanabe, Y. Kobara, K. Baba, and H. Eun, *Anal. Lett.*, 48 (2015) 213.
10. A. Laaniste, I. Leito, R. Rebane, R. Lõhmus, A. Lõhmus, F. Punga, and A. Kruve, J*ournal of Environmental Science and Health*, *Part B*, 51 (2016) 455.
11. M. Pastor-Belda, I. Garrido, N. Campillo, P. Viñas, P. Hellín, P. Flores, and J. Fenoll, *Food Chemistry*, 202 (2016) 389.
12. G. Li, X. Li, and X. Chen, *Asian Journal of Chemistry*, 27 (2015) 3647.
13. Y. Wang, W. Bai, and Z. Cui, *Spectroscopy Letters*, 48 (2015) 259.
14. Z.J. Papp, V.J. Guzsvány, S. Kubiak, A. Bobrowski, and L. Bjelica, *J. Serb. Chem. Soc*, 75 (2010) 681.
15. V. Urbanová, A. Bakandritsos, P. Jakubec, T. Szambó, and R. Zbořil, *Biosensors and Bioelectronics*. 89 (2017) 532.
16. Đorđević, J.S., V.M. Maksimović, S.B. Gadžurić, and T.M. Trtić-Petrović, *Analytical Letters*, 2016 (just-accepted).
17. E. Menart, V. Jovanovski, and S.B. Hočevar, *Electrochemistry Communications*, 2015. 52 (2015) 45.
18. C. Sengiz, G. Congur, and A. Erdem, *Sensors*, 15 (2015) 22737.
19. E. Omidinia, S.M. Naghib, A. Boughdachi, P. Khoshkenar, and D.K. Mills, *Int. J. Electrochem. Sci.*, 10 (2015) 6833.
20. A. Salimi, B. Pourbahram, S. Mansouri-Majd, and R. Hallaj, *Electrochim. Acta*, 156 (2015) 207.
21. J. Tashkhourian, M. Daneshi, F. Nami-Ana, M. Behbahani, and A. Bagheri, *Journal of Hazardous Materials*, 318 (2016) 117.
22. C. Yang, M.E. Denno, P. Pyakurel, and B.J. Venton, *Analytica Chimica Acta*, 887 (2015) 17.
23. J. T. Mehrabad, M. Aghazadeh, M. R. Ganjali, P. Norouzi, *Mater. Lett.,* 184 (2016) 223.
24. I. Karimzadeh, M. Aghazadeh, T. Dourudi, M. R. Ganjali, and P. H. Kolivand *Curr. Nanoscience,* 13 (2017) 167.

25. M. Aghazadeh, M. G. Maragheh, M. R. Ganjali, and P. Norouzi, *Inorganic and Nano-Metal Chemistry* 27 (2017) 1085.
26. S. Tajik, M.A. Taher, and H. Beitollahi, *Sens. Actuators B*, 197 (2014) 228.
27. M. Aghazadeh, M. R. Ganjali, *J Materials Science Materials in Electronics,* 28 (2017) 8144.
28. I Karimzadeh, M Aghazadeh, M. R. Ganjali, P Norouzi, and T Doroudi, *Mater. Lett*, 189 (2017) 290.
29. M.R. Akhgar, H. Beitollahi, M. Salari, H. Karimi-Maleh, and H. Zamani, *Anal. Methods*, 4 (2012) 259.
30. M. Aghazadeh, I. Karimzadeh, M. R. Ganjali, M. M. Morad, *Mater. Lett.* 196 (2017) 392.
31. M. Aghazadeh, M. Asadi, M. R. Ganjali, P. Norouzi, B. Sabour, and M. Emamalizadeh, *Thin Solid Films* 634 (2017) 24.
32. H. Karimi-Maleh, M.R. Ganjali, P. Norouzi, A. Bananezhad, *Materials Science and Engineering C* 73 (2017) 472.
33. H. Beitollahi, J.B. Raoof, H. Karimi-Maleh, R. Hosseinzadeh, *Journal of Solid State Electrochemistry*, 16 (2012) 1701.
34. P. Norouzi, H. Haji-Hashemi, B. Larijani, M. Aghazadeh, E. Pourbasheer and M. R. Ganjali, *Curr. Anal. Chem.*, 13 (2017) 70.
35. P. Norouzi, I. Alahdadi, and S.J. Shahtaheri, *Int. J. Electrochem. Sci,* 10 (2015) 3400.
36. P. Norouzi, V. K. Gupta, B. Larijani, S. Rasoolipour, F. Faridbod and M. R. Ganjali, *Talanta*, 131, (2015) 577.
37. P. Daneshgar, P. Norouzi, M.R. Ganjali, A. Ordikhani-Seyedlar, and H. Eshraghi, *Colloids and Surfaces B: Biointerfaces*, 68 (2009) 27.
38. P. Norouzi, B. Larijani, M. R. Ganjali and F. Faridbod, *Int. J. Electrochem. Sci.*, 9 (2014) 3130.
39. P. Norouzi, B. Larijani, F. Faridbod and M. R. Ganjali, *Int. J. Electrochem. Sci,* 8 (2013) 6118.
40. P. Daneshgar, P., P. Norouzi, M.R. Ganjali, and H.A. Zamani, *Talanta*, 77 (2009) 1075.
41. V.K. Gupta, P. Norouzi, H. Ganjali, F. Faridbod, and M.R. Ganjali, *Electrochimica Acta*, 100 (2013) 29.
42. X. Sun, Z. Liu, K. Welsher, J.T. Robinson, A. Goodwin, S. Zaric, and H. Dai, *Nano Research,* 1 (2008) 203.
43. A. Wojcik, and P.V. Kamat, *ACS nano,* 4 (2010) 6697.
44. P. Zhao, P., N. Li, and D. Astruc, *Coordination Chemistry Reviews*, 257 (2013) 638.
45. S. Jafari, F. Faridbod, P. Norouzi, A. S. Dezfuli, D. Ajloo, F. Mohammadipanah and M. R. Ganjali, *Anal. Chim. Acta*, 895 (2015) 80.
46. P. Norouzi, M.R. Ganjali, and A.E. Meibodi, *Analytical Letters*, 41 (2008) 1208.
47. P. Norouzi, P., B. Larijani, M. Ganjali, and F. Faridbod, Int J Electrochem Sci, 7 (2012) 10414.
48. P. Norouzi, M. R. Ganjali, and P. Matloobi, *Electrochem. Commun.*, 7 (2005) 333.
49. P. Daneshgar, P. Norouzi, and M.R. Ganjali, *Sensors and Actuators B: Chemical*, 136 (2009) 66.
50. P. Norouzi, M. R. Ganjali, and L. Hajiaghababaei, *Anal. Lett.,* 39 (2006) 1941.
51. P. Norouzi, M. R. Ganjali, A. Sepehri, and M. Ghorbani, *Sens. Actuators B*, 110 (2005) 239.
52. V.J. Guzsvány, F.F. Gaál, L.J. Bjelica, S.N. Ökrész, *J. Serb. Chem. Soc.*, 5 (2005) 735.
53. V. Guzsvány, M. Kádár, F. Gaál, L. Bjelica and K. Tóth, *Electroanalysis*, 18 (2006) 1363.
54. A. Kumaravel and M. Chandrasekaran, *Sensors and Actuators B: Chemical*, 174 (2012) 380.
55. M. Putek, V. Guzsvány, B. Tasić, J. Zarębski, and A. Bobrowski, *Electroanalysis*, 24 (2012) 2258.
56. P. Chorti, J. Fischer, V. Vyskocil, A. Economou, and J. Barek, *Electrochimica Acta* 140 (2014) 5.
57. V. Urbanová, A. Bakandritsos, P. Jakubec, T. Szambó, and R. Zbořil, *Biosensors and Bioelectronics,* 89 (2017) 532.